CHAPTER 9

PERFORMANCE OF THE INTERFEROMETER

"Deus ex machina."
("A god from the machine.")
Menander

9.1 ASSESSMENT OF THE INTERFEROMETER

One major problem in assessing the performance of the interferometer is that there is no other instrument or set of calibrated length bars at NPL with sufficient accuracy against which comparisons can be made over the full range of the new instrument. Other NPL instruments which can be used for length bar measurements are: the NPL Length Bar Machine (bars 100 mm - 1200 mm, uncertainty ± 68 ± 350L nm), the National Standard Multi-axis Co-ordinate Measuring Machine (uncertainty approximately ± 100 - 300 nm), and the NPL Gauge Block Interferometer (length bars 25 - 300 mm, uncertainty ± 24 ± 480L nm, L in metres). The only instrument capable of similar accuracy is the Kösters-Zeiss interferometer operated by PTB (Physikalisch Technische Bundesanstalt) - the German national standards laboratory. For brevity, the following acronyms will be used to describe the NPL instruments:

GBI Gauge Block Interferometer
LBM Length Bar Machine
LBI Length Bar Interferometer (the subject of this thesis)

An intercomparison of long series gauge blocks of lengths 600 mm and 1000 mm is planned to take place in 1994, under the auspices of EUROMET. The new Length Bar Interferometer will take part in this intercomparison, as well as the Length Bar Machine. Until this date, NPL has only one length bar that has been measured elsewhere. This is a 36 inch master standard, used as a checking standard in the Length Bar Machine. This bar was measured at PTB in 1988, with results for central length and thermal expansion coefficient. Unfortunately, the faces of the bar have become scratched and pitted, necessitating them being re-lapped, thus shortening the bar. The thermal expansivity is however unaffected and so this bar is useful as a thermal expansion standard.

Chapter 10 contains a full uncertainty analysis for length measurements made by the interferometer - this is the theoretical uncertainty which can be achieved by the interferometer. Unless there is evidence to the contrary, this will be the reported performance of the instrument.

To see whether this level of performance is achieved in practice, a set of length bars (NPL set 1455) has been measured on all available equipment. The set has been measured twice in the LBM and GBI (100 - 1200 mm and 25 - 300 mm respectively) and twice in the LBI, with a gap of approximately one year between the repeated measurements. Measurements of thermal expansion have been made for the 36 inch standard and a group of bars from set 1455. Measurements have also been made with "zero-length" objects, *i.e.* the platen with no bar wrung to it, to assess the accuracy of the optics and the fringe fraction measurement. Thin film fringe fraction samples have also been measured - these are optical glass flats, coated with chromium, with a step height at the centre, in the shape of a gauge block, with a height of less than one fringe. These have been manufactured using thin film deposition techniques and etching.

9.2 FRINGE FRACTION MEASUREMENTS

Two different results have been obtained for the measurements of the thin film fringe fraction samples using the two available data-fitting procedures: Chebychev surface (CS) and best fit plane (BFP). The BFP algorithm is a simple least-squares fit of a plane ($z = ax + by + c$) to the phase data of the platen (for each wavelength). The CS analysis simply fits Chebychev polynomials on a line-by-line basis to 127 horizontal lines through the data. The individual lines are not connected with each other. A full least-squares surface fit, of the form $z = ax + by + cx^2 + dy^2 + e$ will be programmed, when time permits. The two procedures produce slightly different results, depending on the flatness of the platen surface: both will fit well to flat platens, whereas the BFP algorithm will depart from the CS for curved platen surfaces. The answer to the question of which is correct depends on the exact definition of the length of the bar. British Standard BS 5317 simply states that the length is the distance between the centre of the face and a flat surface in wringing contact with the other end. The degree of flatness of the platen is not specified, nor the way in which the corresponding platen surface is determined from the measured data. Due to size/weight considerations, the platens have to be relatively thin, and they are supported by wringing, rather than using proper kinematic supports, and so good flatness is difficult to achieve. Typical flatness of the wrung platens is $\lambda/20$. It is up to the operator to select the desired analysis and to interpret the results. It should be noted however, that the errors due to the data fitting are scaled according to the wavelength - they have the same effect on all three phase

maps, and hence do not influence the choice of nominal order in the multiple-wavelength analysis.

The fringe fraction samples were measured in the Gauge Block Interferometer and in the new interferometer. The GBI uses a best fit least-squares surface, the new interferometer used both CS and BFP analyses.

Fringe fraction measurement (λ = 633 nm)		
GBI	LBI (BFP)	LBI (CS)
0.313	0.310	0.277
0.647	0.663	0.651

Table 9.1 *- Fringe fraction sample results (mean of 50 measurements) BFP - Best Fit Plane, CS - Chebychev Surface*

The results using the BFP analysis are in better agreement with the GBI than the Chebychev Surface results. This is because the GBI uses a similar analysis technique. Due to the optical adjustments required to image these samples properly in the new interferometer, the fringe fractions are not measured at the same position as in the GBI. Both samples are out of flat by at least 0.1 fringe (32 nm) thus some differences between fringe fractions measured in the GBI and the LBI should be expected. Considering only the BFP measurements, the GBI and LBI are in agreement to within 0.016 fringe (5 nm).

9.3 ZERO-LENGTH MEASUREMENTS

The results of the zero-length measurements (measurements of platen surfaces with nothing wrung on) are similarly affected by the choice of analysis. Platen number 1 was selected as being the flattest and least scratched of the six interferometer platens. Fifty measurements were made of the platen using both analysis types. The mean results, spread in the results, and the standard deviation are given in table 9.2. These were measured using the mask set up for a length bar, *i.e.* the central region of the phase data is taken to correspond to the surface of the bar, with the surrounding region corresponding to the platen. For a totally flat platen, the measured length should be zero.

Analysis	Mean (nm)	Spread (nm)	Std Devn (nm)
BFP	+ 24.1	3	0.44
CS	+ 6.36	4	0.56

Table 9.2 *- Results of zero-length measurements*

The two techniques agree on the flatness of the platen as 53 nm (± 2 nm) over the area where the bar would be wrung. The BFP analysis is not suitable for a measurement such as this where the platen is not flat. The CS analysis consistently resulted in a measured length of 6.36 nm, with a spread of 4 nm. This corresponds to a fringe fraction of 0.020 for the red wavelength.

9.4 CENTRAL LENGTH MEASUREMENTS

The measurements of bars from set 1455 were all performed using chebychev surface analysis because this provides more accurate results than the BFP analysis for non-flat platens. The bars were measured both ways round, *i.e.* with the platen wrung to each face in turn. The quoted result is the difference between the mean of these two measurements and the nominal size of the bar, *i.e.* it is the departure from nominal length. The results for the GBI and LBM are also means of two orientations. The difference between the 1st and 2nd wringing results (|FW - SW|) for the LBI is given.

The results of the GBI have been corrected to the horizontal position, allowing for prismatic compression of the bar under its own weight (see Appendix D).

Nominal length (mm)	Deviation from nominal (nm)	Difference in LBI results | FW - SW | (nm)	LBI -LBM (nm)	LBI -GBI (nm)
100	1666	2	76	59
125	-313	14	-5	-47
150	-571	11	-2	21
175	457	3	27	8
200	125	*	33	1
225	613	3	25	53
250	-926	27	34	-6
275	-449	2	23	70
300	343	10	159	50
400	-1125	64	70	N/A
500	1170	42	69	N/A
600	-1454	31	37	N/A
700	2172	19	161	N/A
800	-776	12	24	N/A
900	452	12	11	N/A
1000	3555	22	-77	N/A
1200	5362	8	108	N/A

** The 200 mm bar could only be wrung one way round due to a burr*

***Table 9.3** - Comparison results of length bars measured in three instruments*

The differences between the results are graphed in figure 9.1.

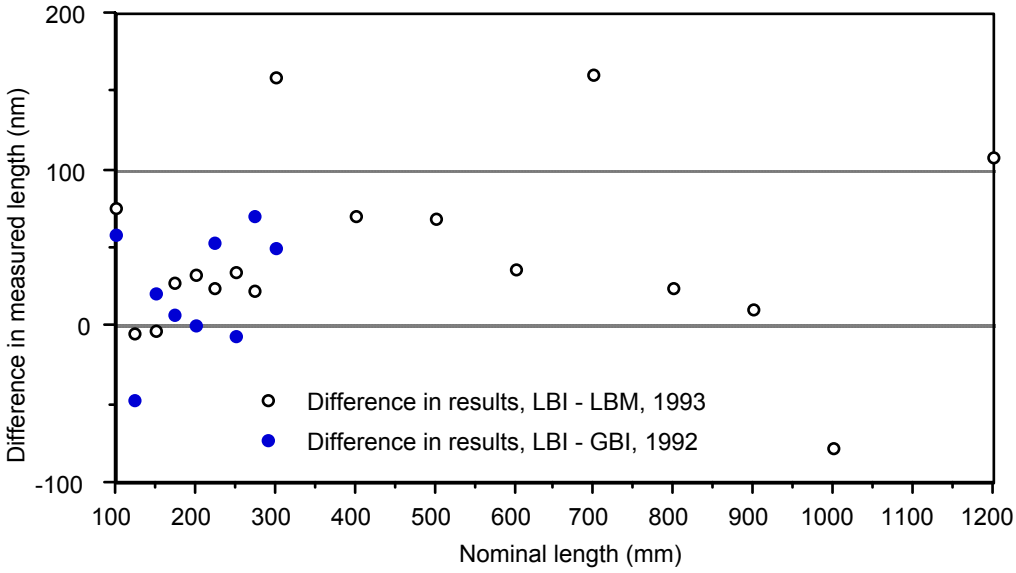

Figure 9.1 *- Comparison of length bar measurements from three instruments*

A full uncertainty budget for the Length Bar Interferometer is given in chapter 10. The uncertainty for central length measurements is approximately ± 30 nm ± 64 L nm, where L is the length of the bar, in metres. The uncertainty budget for the GBI, adapted for length bars, is approximately ± 54 nm ± 480 L nm. All the differences between the results of the GBI and the LBI fall within the uncertainty budget of the GBI alone. The uncertainty budget for the LBM is approximately ± 68 nm ± 350 L nm. All of the differences between the results of the LBM and the LBI fall within the uncertainty budget of the LBM alone, except for the 300 mm bar. Both the LBM and LBI give repeatable results for this bar which are different by approximately 160 nm. The bar is however not particularly flat and is out of tolerance on parallelism (variation in length) and so some of this discrepancy could be due to the LBM probing the surface in a slightly different place from the LBI (possibly 1 mm separation). The LBI result is a mean of 81 pixels at the centre of the optical face of the bar, whereas the LBM result is a single point contact with the mechanical surface. The poor flatness and parallelism could cause distortion of the platen when wringing, resulting in difference between the two instruments.

The results of the LBM are all consistently longer than the results for the same bars measured one year ago, except for the 700 mm bar, which appears to be shorter by 122 nm. This bar also displays a larger than expected difference between the LBM and LBI results indicating a possible error in the LBM result. The results of the LBI are all consistently shorter than the results for the same bars measured one year ago, except for the 100 mm, 125 mm and 300 mm bars.

Although the result for the 100 mm bar is within the uncertainty budget, there is a significant difference between the LBM and LBI results. This is thought to be due to lifting of the bar when contacted by the LBM probes - the weight of the bar is insufficient to keep it in place on the supports when probed. This effect, which has also been observed with other short bars in the LBM, would constitute a cosine error in the length measurement.

9.5 FLATNESS & PARALLELISM MEASUREMENTS

Some example results of flatness and parallelism measurements were given in figure 6.16. Additionally, 100 repeated measurements have been made of length bars sized 125 mm and 900 mm.

Results in fringes (633 nm)		Mean	Spread	Std Deviation
125 mm	Flatness	0.359	0.04	0.0086
	Parallelism	0.539	0.04	0.0090
900 mm	Flatness	0.224	0.05	0.0106
	Parallelism	0.375	0.05	0.0096

Table 9.4 *- Flatness and parallelism results after repeated measurement*

Repeatability of flatness and parallelism measurements is within 0.05 fringe (16 nm). The repeatability after the bar is re-wrung and re-measured depends on the quality of the wringing and the positioning of the software cursors, but is similar to the figures in table 9.4.

Figure 9.2 shows a typical screen display (this photograph was taken when the software was still in development and so some of the details have since changed). The screen displays information about the bar down the left side of the image. The red fraction and green fraction (also now the orange fraction) are the measured fringe fractions used in the multiple-wavelength analysis. The Peak and Valley results (now combined as Variation) are the maximum and minimum values of the fringe fraction across the surface of the bar. The calculated length is the length of the bar calculated from the two (now 3) fringe fractions, corrected to 20 °C. The departure is the difference between the measured length and the nominal length input by the user. Down the right side of the display are (top) the phase map (λ = 633 nm) in a colour representation with scale to the right hand side, and (below) the phase map in a pseudo-three-dimensional display. Note the area which has been masked off shown as dark blue in the upper display and seen as the flat area surrounding the bar in the lower display.

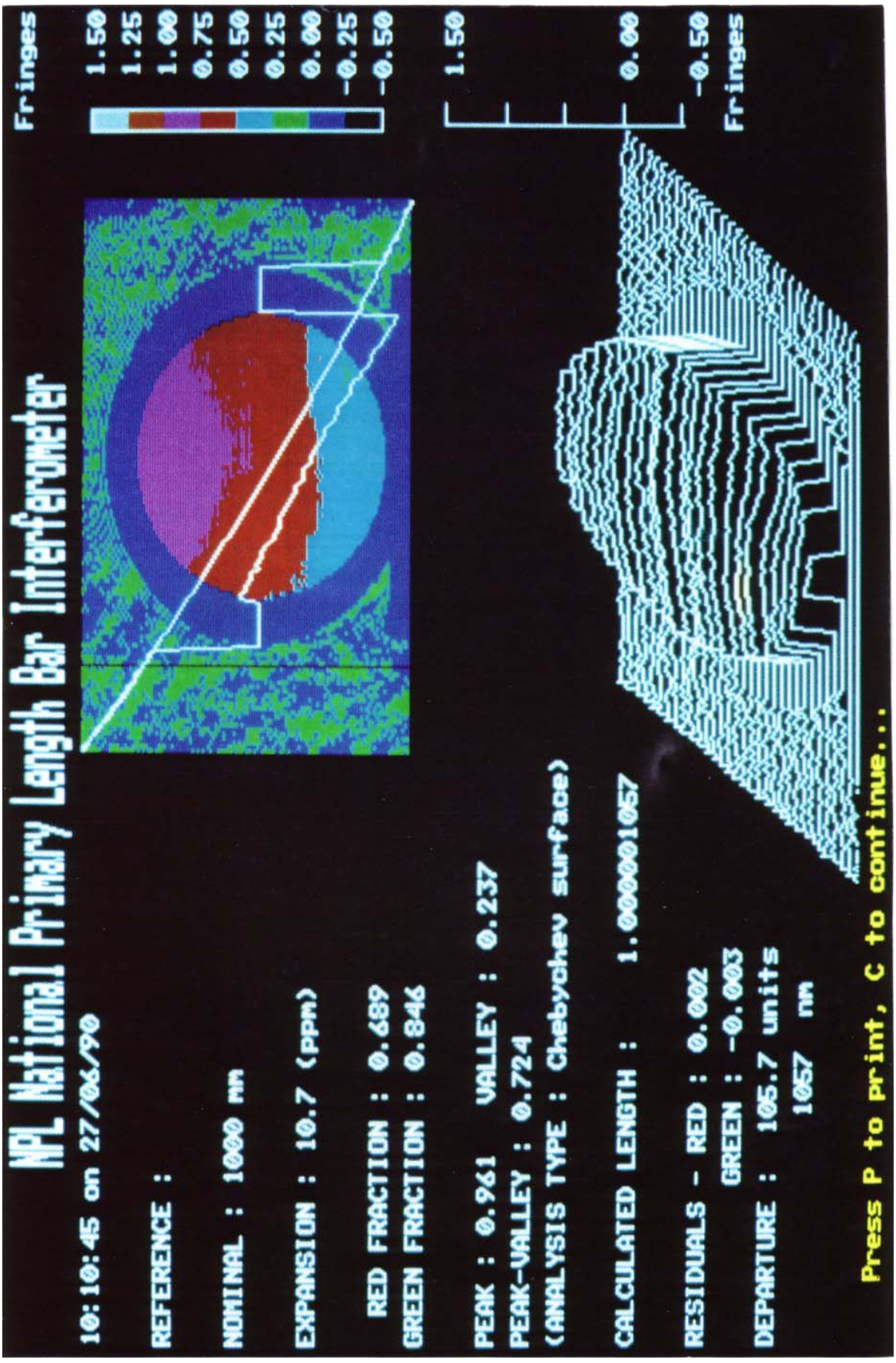

Figure 9.2 *- Photograph of screen showing results for a 1000 mm length bar (using a previous version of the software)*

9.6 THERMAL EXPANSION MEASUREMENTS

Measurements of thermal expansion have been performed for 6 length bars over the range 100 mm to 1m. The bars were measured at a minimum of 5 different temperatures over the range 20 °C - 30 °C. At each temperature, the alignment of the interferometer was checked using the return-spot technique and the interferometer allowed to stabilise at the correct temperature. Each bar was measured in one orientation only. The bars were selected from NPL set 1455. The data of the measured lengths and temperatures were entered into *Mathematica*, and a least squares quadratic fit was determined. This was of the form $L_{20}\,(1 + \alpha\,(T\text{-}20) + \beta\,(T\text{-}20)^2)$, where L_{20} is the length at 20 °C, α is the linear coefficient of thermal expansion, β is the second order coefficient of thermal expansion, and T is the temperature of the bar in °C.

100 mm bar

Bar temperature (°C)	Bar Length (mm)
20.006	100.001 689
22.061	100.004 039
23.927	100.006 194
26.035	100.008 630
28.117	100.011 048
29.996	100.013 237

L_{20} = 100.001 680 mm, α = 11.442 x 10^{-6} K^{-1} and β = 12.0 x 10^{-9} K^{-2}

125 mm bar

Bar temperature (°C)	Bar Length (mm)
20.006	124.999 718
22.067	125.002 471
23.941	125.004 996
26.046	125.007 843
28.130	125.010 664
10.167	125.013 437

L_{20} = 124.999 707 mm, α = 10.694 x 10^{-6} K^{-1} and β = 10.8 x 10^{-9} K^{-2}

225 mm bar

Bar temperature (°C)	Bar Length (mm)
20.006	225.000 620
21.887	225.005 130
24.711	225.011 897
27.734	225.019 188
30.037	225.024 743

L_{20} = 225.000 607 mm, α = 10.630 x 10^{-6} K^{-1} and β = 5.8 x 10^{-9} K^{-2}

500 mm bar

Bar temperature (°C)	Bar Length (mm)
20.008	500.001 270
21.884	500.011 279
24.715	500.026 408
27.702	500.042 463
30.008	500.054 879

L_{20} = 500.001 229 mm, α = 10.650 x 10^{-6} K^{-1} and β = 7.2 x 10^{-9} K^{-2}

900 mm bar

Bar temperature (°C)	Bar Length (mm)
20.006	124.999 718
22.067	125.002 471
23.941	125.004 996
26.046	125.007 843
28.130	125.010 664
30.051	900.097 523

L_{20} = 900.000 570 mm, α = 10.633 x 10^{-6} K^{-1} and β = 8.6 x 10^{-9} K^{-2}

1000 mm bar

Bar temperature (°C)	Bar Length (mm)
20.009	1000.003 679
21.896	1000.023 850
24.719	1000.054 058
27.727	1000.086 357
30.034	1000.111 151

L_{20} = 1000.003 580 mm, α = 10.678 x 10^{-6} K^{-1} and β = 4.2 x 10^{-9} K^{-2}

Whilst there is no obvious length dependency of the α and β coefficients, it is the two shortest bars which have the largest β coefficients and the 100 mm bar has a markedly larger α coefficient than the other bars, indicating that this bar has perhaps had a different hardening treatment than the others. Whether the β coefficient as measured is a real second-order non-linearity is difficult to say conclusively, since the calculated uncertainties of the α and β values are of the order of $\pm 10^{-8}$. Thus the apparent non-linearity could be due to temperature dependent errors in the length measurement.

All these bars were measured using a nominal coefficient of $\alpha_{nom} = 10.7 \times 10^{-6}\ K^{-1}$. The above results show that this value was not exactly correct for each bar, however the scanning range of the interferometer was sufficient to cope with this and was able to select the correct solution in the multiple-wavelength analysis.

To confirm the accuracy of these results for α and β, the 36 inch standard length bar previously measured at PTB was measured in the PLBI. The PTB result was:

$$L = 914.4\ \text{mm} - 1.04\ \mu\text{m} + 9.887\ (T\text{-}20)\mu\text{m} + 0.005\ (T\text{-}20)^2\mu\text{m} \qquad (10.1)$$

or

$$\alpha = 10.813 \times 10^{-6}\ K^{-1},\ \beta = 5.5 \times 10^{-9}\ K^{-2} \qquad (10.2)$$

$$(\pm\ 0.0065 \times 10^{-6}\ K^{-1},\ \pm\ 2 \times 10^{-9}\ K^{-2})$$

The result from the PLBI was:

$$\alpha = 10.798 \times 10^{-6}\ K^{-1},\ \beta = 6.5 \times 10^{-9}\ K^{-2} \qquad (10.3)$$

$$(\pm\ 0.012 \times 10^{-6}\ K^{-1})$$

The results for α agree within the measurement uncertainties of the two instruments. The β results are also in close agreement. The length of the bar is not quoted for the PLBI because the bar was re-lapped in 1992 to remove surface irregularities, and was found to be approximately 2 μm shorter than in 1988.

The 100 mm and 125 mm length bars were independently measured in the NPL Gauge Block Dilatometer (GBD) [**1**,**2**]. This is a Fizeau interferometer under development at NPL for the measurement of the thermal expansion coefficient of gauge blocks. Unfortunately the results obtained by the GBD for the 100 mm and 125 mm bars were inconclusive because the GBD software had difficulty measuring accurate fringe

fractions - the optics were designed for gauge blocks, not length bars which leave very little of the platen visible for accurate interpolation.

9.7 GAUGE BLOCK MEASUREMENTS

Although the principles of operation are the same for gauge block and length bar measurement, an example of a gauge block measurement is included here for comparison. The main difference is the shape of the mask is now rectangular rather than circular and the image magnification has been decreased to fit the image of the end of the gauge into the imaging plane (see § 3.2.4).

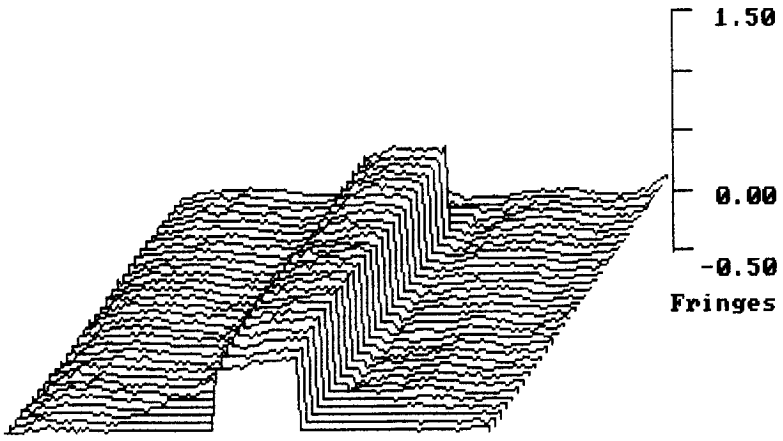

Figure 9.3 *- Example measurement of a gauge block*

9.8 DOUBLE-ENDED MEASUREMENTS

When the optics are adjusted for double-ended imaging (smaller magnification, carriage displaced laterally, length bar supported at exactly the Airy points), the image digitised into the framestore is similar to that shown in figure 9.4. The right image is the front face of the bar, the left image is the other end of the bar, which would normally be wrung to the platen. After the phase-stepping , discontinuity-removal and surface-fitting have been performed, the resultant 3 phase maps are as shown in figure 9.5.

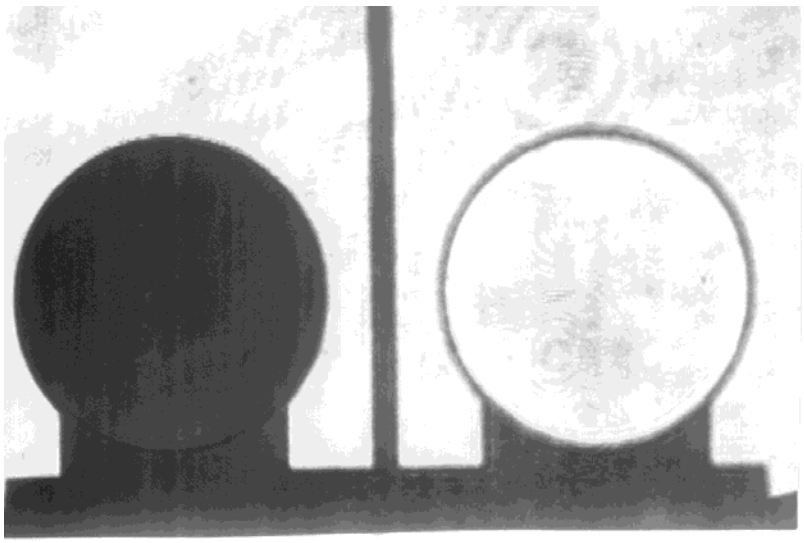

Figure 9.4 *- Double-ended image, stored in framestore during measurement*

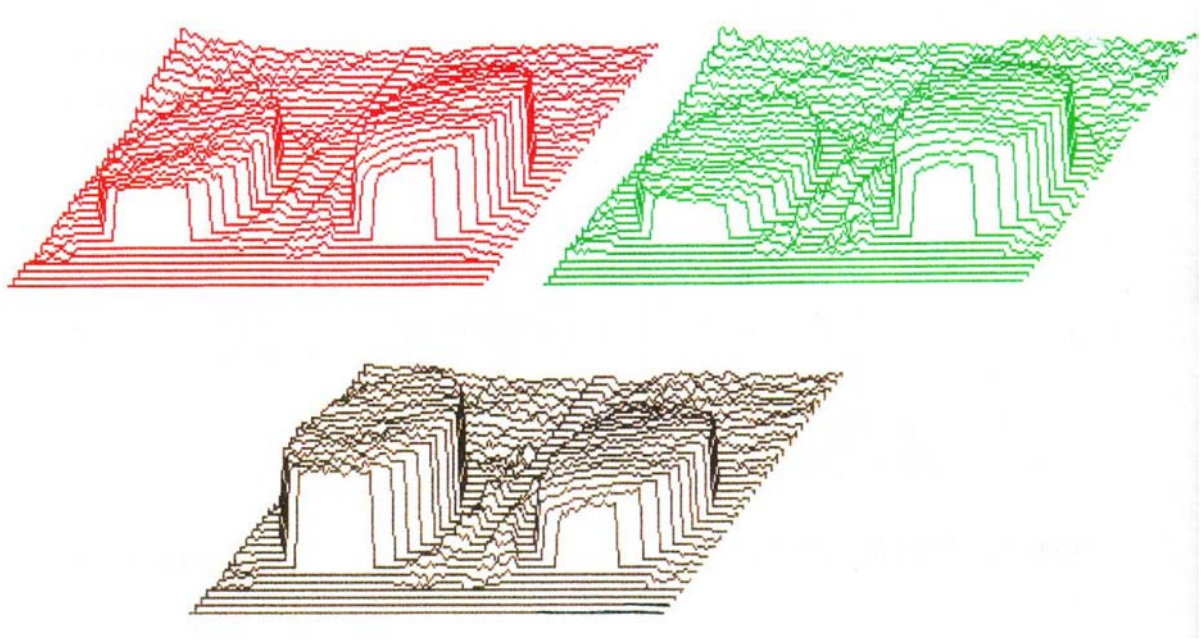

Figure 9.5 *- Three phase maps obtained during a double-ended measurement*

As shown in figure 9.5, the phase data in the background area of the image is very noisy due to the reduced fringe contrast, visible in figure 9.4 (and more apparent in figure 4.23). Also, the amount of background data available for use in the surface-fitting is much less than in the analysis used with wrung bars, so the fitting of a least-squares plane is less accurate. Any mis-match between the two orthogonal mirrors will appear as extra tilt in either of the 2 sides of the background data, leading to further reduced accuracy in the least-squares plane fitting. For these reasons it has not been possible to measure fringe fractions with sufficient accuracy to use the double-ended multiple-wavelength calculation.

9.9 CONCLUSIONS ON PERFORMANCE

The differences between the measurements of the fringe fraction samples on the LBI and GBI are within 0.016 fringes at $\lambda = 633$ nm. This is similar to the mean of the zero-length measurements implying that the uncertainty in the processed fringe fraction measurements is similar to this, hence a value of ± 0.016 fringes or ± 5 nm will be assumed for the accuracy of the fringe fractions measured by the interferometer in the overall uncertainty budget in chapter 10. In § 5.4 it was shown that the errors due to the phase-stepping are smaller than this so the limiting factor must be the data analysis surface-fitting. Hopefully this will be improved when the least-squares best fit surface is programmed or by using flatter platens.

The flatness and parallelism results are repeatable to within 0.05 fringe (16 nm). It is expected that the parallelism (variation) results are better than the flatness results as the latter requires further data fitting of a least-squares plane, whereas the former uses the data directly.

The intercomparison between the 3 instruments shows that the results for all 3 instruments are within their respective uncertainty budgets. This does not confirm that the uncertainty budgets are exactly correct, but that they are not too small. With more measurements one would expect that 5% of the readings would be outside the uncertainty budgets because they are at the 95% confidence level.

The new interferometer performs as expected and the variation in results is within the uncertainty budget derived in chapter 10.

REFERENCES FOR CHAPTER 9

[**1**] Hughes E B NPL Gauge Block Dilatometer - *MSc dissertation* Brunel University (1992)

[**2**] Hughes E B Measurement of the thermal expansion coefficient of gauge blocks by interferometry *Proc. SPIE* **2088** (1993) 179-189